JACS
JOURNAL OF THE AMERICAN CHEMICAL SOCIETY
Article
pubs.acs.org/JACS

Real-Time Molecular Imaging of Tricarboxylic Acid Cycle Metabolism in Vivo by Hyperpolarized 1-^{13}C Diethyl Succinate

Niki M. Zacharias,[†,‡] Henry R. Chan,[†] Napapon Sailasuta,[†] Brian D. Ross,[†] and Pratip Bhattacharya*[,†]

[†]Enhanced MR Laboratory, Huntington Medical Research Institutes, Pasadena, California, United States
[‡]Division of Chemistry and Chemical Engineering, California Institute of Technology, Pasadena, California, United States

Supporting Information

ABSTRACT: The Krebs tricarboxylic acid cycle (TCA) is central to metabolic energy production and is known to be altered in many disease states. Real-time molecular imaging of the TCA cycle in vivo will be important in understanding the metabolic basis of several diseases. Positron emission tomography (PET) with FDG-glucose (2-[^{18}F]fluoro-2-deoxy-D-glucose) is already being used as a metabolic imaging agent in clinics. However, FDG-glucose does not reveal anything past glucose uptake and phosphorylation. We have developed a new metabolic imaging agent, hyperpolarized diethyl succinate-*1*-^{13}*C*-*2,3*-d_2 , that allows for real-time in vivo imaging and spectroscopy of the TCA cycle. Diethyl succinate can be hyperpolarized via parahydrogen-induced polarization (PHIP) in an aqueous solution with signal enhancement of 5000 compared to Boltzmann polarization. ^{13}C magnetic resonance spectroscopy (MRS) and magnetic resonance imaging (MRI) were achieved in vivo seconds after injection of 10−20 μmol of hyperpolarized diethyl succinate into normal mice. The downstream metabolites of hyperpolarized diethyl succinate were identified in vivo as malate, succinate, fumarate, and aspartate. The metabolism of diethyl succinate was altered after exposing the animal to 3-nitropropionate, a known irreversible inhibitor of succinate dehydrogenase. On the basis of our results, hyperpolarized diethyl succinate allows for real-time in vivo MRI and MRS with a high signal-to-noise ratio and with visualization of multiple steps of the TCA cycle. Hyperpolarization of diethyl succinate and its in vivo applications may reveal an entirely new regime wherein the local status of TCA cycle metabolism is interrogated on the time scale of seconds to minutes with unprecedented chemical specificity and MR sensitivity.

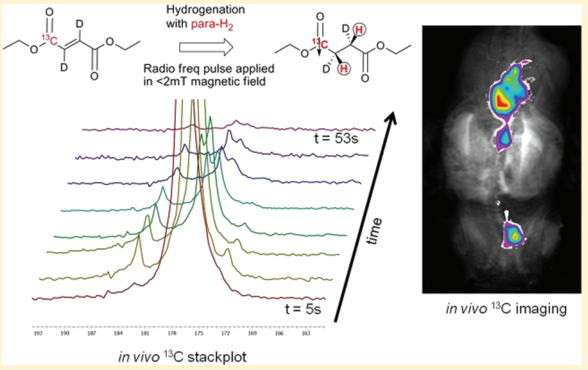

INTRODUCTION

The Krebs tricarboxylic acid cycle (TCA) and oxidative phosphorylation are central to metabolic energy production. The TCA cycle occurs in the mitochondria of cells and in most cells produces the majority of adenosine triphosphate (>90%). In normal cells, the main energy source for the TCA cycle is pyruvate that is generated from glycolysis of glucose.[1] Biochemistry has revealed that many disease states have perturbed TCA cycles. In cancer, TCA cycle succinate dehycrogenase, isocitrate dehydrogenase, and fumarate hydratase oncogenes impair the TCA cycle.[2] The TCA cycle can have different entry points and, especially in cancer, a broad range of energy substrates can be used in the TCA cycle (citrate, glutamate/glutamine).[3] There is evidence that the TCA cycle is altered in many neurodegenerative diseases (Alzheimer's, Parkinson's, Huntington's, and amyotrophic lateral sclerosis).[4−6] Inhibition of succinate dehydrogenase in the brain by the irreversible inhibitor 3-nitropropionate in animals is a model for Huntington's disease, and these animals produce symptoms and lesions similar to those observed in the disease.[7] Many of the metabolic differences between disease and normal tissue can and could be examined through the use of metabolic imaging agents.

Presently, metabolic imaging is routinely done with positron emission tomography (PET) measurements of the uptake of FDG-glucose (2-[^{18}F]fluoro-2-deoxy-D-glucose) or magnetic resonance spectroscopy (MRS). PET imaging with FDG-glucose measures only the level of uptake of glucose and phosphorylation and reveals nothing about the subsequent metabolism of glucose. In MRS, only the steady state of a tissue/organ's metabolic profile can be determined, and due to low signal-to-noise ratio (SNR), the length of the exam can be quite long (^{13}C MRS exam can take hours).[8] The invention of hyperpolarized molecules has opened the way to real-time metabolic imaging in vivo. Hyperpolarization can lead to sensitivity enhancements of >10 000-fold, and the polarization (signal enhancement) can be retained on the metabolites of the hyperpolarized molecule.[9−12] In addition, unlike PET, the process of hyperpolarization is nonradioactive. Hyperpolarization of compounds that can be metabolized in vivo allows for real-time metabolic imaging. The most widely used methods for hyperpolarization are dynamic nuclear polarization (DNP) and parahydrogen-induced polarization (PHIP). The utility of

Received: May 3, 2011
Published: December 7, 2011

 © 2011 American Chemical Society dx.doi.org/10.1021/ja2040865 | J. Am. Chem.Soc. 2012, 134, 934−943

DNP-polarized [1-^{13}C]pyruvate in metabolic imaging has been explored extensively.[13−17] Hyperpolarized [1-^{13}C]pyruvate can be used to follow the metabolism of pyruvate to alanine, lactate, and bicarbonate but reveals nothing about TCA cycle metabolism. Recently, DNP-polarized [2-^{13}C]pyruvate was administered to isolated perfused rat hearts, and hyperpolarized TCA metabolites glutamate and citrate were detected;[18] however, when the hyperpolarized compound was used for metabolic imaging in the brain in vivo, only [2-^{13}C]lactate was detected.[19]

In our laboratory, we recently used the PHIP method to hyperpolarize succinate, 2-hydroxyethyl propionate, and 2,2,3,3-tetrafluoropropyl [1-^{13}C, 2,2,3,3-d_4]propionate (TFPP) for in vivo applications.[20−22] However, all of these compounds currently have physiological barriers to being used in the clinic. For [^{13}C]succinate, the polarization transfer has to be done at acidic pH $\leq$ 3 or alkaline pH $\geq$ 9 for optimum hyperpolarization.[20] It is known that the dicarboxylic acid succinate is poorly transported across many biological membranes and in particular barely crosses the mitochondrial membrane to gain access to TCA cycle enzymes involved in metabolism.[23,24] 2-Hydroxyethyl propionate is toxic and is not metabolized.[21] TFPP is not very water-soluble and has to be injected in a 20% ethanol aqueous solution.[22] We have overcome these hurdles by designing and developing hyperpolarized diethyl succinate. This hyperpolarized compound is better suited for translational research and has potential of being used as a diagnostic imaging agent. We describe the whole development process from synthesis, polarization, and finally in vivo spectroscopy and imaging of the compound and its metabolites in live normal mice.

Diethyl succinate is a neutral molecule, can be used at physiological pH, and crosses biological membranes.[25−28] There is a significant amount of biochemical research on diethyl succinate illustrating the compound's ability to be incorporated into cells in tissue culture and to be metabolized by the TCA cycle.[25,26] In addition, diethyl succinate is known to be nontoxic[29] and is often used in fragrances and flavoring.

The PHIP method uses parahydrogen gas to hydrogenate an unsaturated organic molecule (alkyne or alkene) that is labeled with ^{15}N or ^{13}C.[9,10] A catalyst is used to transfer the hydrogens as a unit on the compound without scrambling the spin state.[11,21,30,31] With diethyl succinate, we transfer the spin order to the ^{13}C-labeled carbonyl by use of radio frequency pulses.[11,32] We generate diethyl [1-^{13}C, 2,3-d_2]succinate by hydrogenation of diethyl [1-^{13}C, 2,3-d_2]fumarate (Figure 1). The hydrogenation and polarization transfer are done in our home-built PHIP polarizer, which is described in detail elsewhere.[33] After diethyl succinate is hyperpolarized, the compound is injected into a mouse or is used as a phantom and ^{13}C spectroscopy and imaging are performed. The PHIP method of hyperpolarization is significantly faster than the DNP method. Each sample of hyperpolarized diethyl succinate requires 4 s for polarization transfer, and an injectable hyperpolarized sample can be generated every 3−4 min (in contrast to the 90 min or more required for hyperpolarization of compounds by DNP).[33,34] In these experiments diethyl [1-^{13}C, 2,3-d_2]fumarate was hydrogenated by parahydrogen and rhodium catalysis to diethyl [1-^{13}C, 2,3-d_2]succinate and hyperpolarized to 2.1% + 0.6% or 5000-fold signal enhancement compared to Boltzmann polarization before tail-vein injection (iv) or intraperitoneal injection (ip) into mice.

The biodistribution and metabolic fate of hyperpolarized [^{13}C]succinate was followed in a specifically equipped MR scanner to provide images and spectra in the first 2 min after injection. Different hyperpolarized metabolites of diethyl succinate were detected. Metabolism was seen in all 13 mice injected with hyperpolarized diethyl succinate by either iv or ip injection. On the basis of published work and our data, after

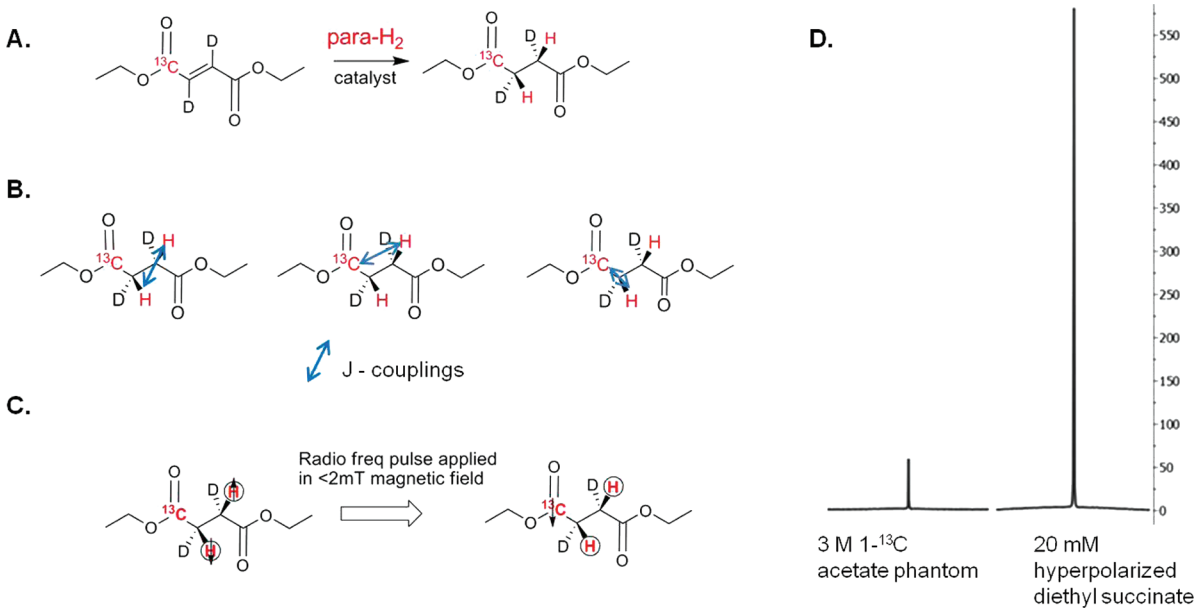

Figure 1. Hydrogenation and polarization. (A) Schematic of hydrogenation of diethyl [1-^{13}C, 2,3-d_2]fumarate to diethyl [1-^{13}C, 2,3-d_2]succinate with parahydrogen (para-H_2) by use of a rhodium bisphosphine catalyst. (B) Coupling constants of diethyl succinate that are needed to create the heteronuclear radio frequency pulse for polarization transfer to ^{13}C atom. (C) Schematic of the polarization transfer from the parahydrogen to the ^{13}C nucleus by use of a radio frequency pulse applied in a low magnetic field. (D) Magnitude of a 20 mM hyperpolarized diethyl succinate ^{13}C signal compared to that from a 3 M [1-^{13}C]acetate phantom. Each spectrum was taken with a single transient. The ratio of the integrated hyperpolarized signal over the value of the acetate signal is used to determine the percentage of polarization. Hyperpolarization of diethyl succinate leads to 5000-fold sensitivity enhancement over Boltzmann polarization.

dx.doi.org/10.1021/ja2040865 | J. Am. Chem.Soc. 2012, 134, 934−943

injection into a mouse, hyperpolarized diethyl succinate is entering cells, the ester functionality is hydrolyzed by esterase, and hyperpolarized succinate is then metabolized in the TCA cycle. We further verified this result by monitoring metabolism of hyperpolarized diethyl succinate in vivo before and after the animal was treated with 3-nitropropionate, a known irreversible inhibitor of succinate dehydrogenase.[35,36] Using ^{13}C true FISP (fast imaging with steady-state precession)[37] imaging, we can determine the relative location of hyperpolarized diethyl succinate and its hyperpolarized metabolites in vivo.

On the basis of our results, we feel that hyperpolarized diethyl succinate has the potential of allowing for direct monitoring in real-time metabolism in vivo. In addition, unlike DNP-hyperpolarized [1-^{13}C]pyruvate, where only single-step metabolism can be visualized,[13−17] hyperpolarized diethyl succinate allows metabolic imaging of multiple steps of the TCA cycle. The metabolism of cells is known to be affected in many diseases, and direct monitoring of metabolism in vivo has the potential of being an excellent diagnostic tool for early detection of diseased tissue and monitoring the success of therapy.

MATERIALS AND METHODS

Parahydrogen. Commercially available ultrapure hydrogen (Gilmore, South El Monte, CA) was catalytically converted to parahydrogen (para-H_2) by slow passage over granular hydrous ferric oxide (IONEX-type O−P catalyst; Molecular Products Inc., Lafayette, CO) at a temperature of 36−55 K. After the gas was converted to parahydrogen, it was stored in 7 L aluminum cylinders at room temperature at a pressure of 33 bar. The quality of para-H_2 was determined to be >90% by high-resolution NMR.[34] Each batch was used within 2 days, during which there was no measurable decrease in the yield.

Synthesis of Diethyl [1-^{13}C, 2,3-$^{2}H_2$]Fumarate. The synthetic method for esterification found in ref38 was used with slight changes. In a dry 150 mL round-bottom flask with stir bar, 1 g (8.44 mmol) of [1-^{13}C, 2,3-d_2]fumaric acid (99% 1-^{13}C, 98% 2,3-d_2, CDLM-6062-0, Cambridge Isotopes, Andover, MA) was added. Then 60 mL of anhydrous ethanol and 3.2 mL (25.2 mmol) of chlorotrimethylsilane (386529, Sigma−Aldrich, St. Louis, MO) was added via syringe into the reaction. Reaction was stirred at room temperature overnight under an inert atmosphere. Reaction was quenched with 20 mL of saturated sodium bicarbonate solution, and solid bicarbonate was added until the solution became neutral. Solution was filtered to remove excess bicarbonate, and ethanol was removed by rotary evaporation. Product was extracted out of aqueous solution with 3 × 25 mL of dichloromethane. Organic layers were combined, dried over anhydrous sodium sulfate, and filtered; the solvent removed by evaporation and 1.10 g (75% yield) of pure product was isolated as a colorless liquid. ^{1}H (CD_2Cl_2, 500 MHz) δ 4.23 (complex quartet, J = 7.1, 1.5, 1.6 Hz, 4H), 1.29 (t, J = 7.1 Hz, 6H). Proton-decoupled ^{13}C NMR (CD_2Cl_2, 125 MHz) δ 165.43 (s), 133.6 (sextet J = 25 Hz, t J = 25 Hz), 61.8 (s), 14.43 (s).

PHIP Hydrogenation. A full description of the equipment used to develop high levels of ^{13}C polarization by use of parahydrogen is given elsewhere,[33] together with details of quality assurance procedures for achieving these levels of polarization reproducibly and routinely.[34]

A water-soluble rhodium catalyst developed for the purpose of rapid hydrogenation while preserving the desired spin order was freshly prepared by mixing two components.[21,31] The bisphosphine ligand, 1,4-bis-[(phenyl-3-propanesulfonate)-phosphine]butane disodium salt (Q36333, Isotec), was dissolved in 9:1 water/D_2O to yield 8.25 mM concentration, followed by removal of oxygen via vacuum and argon purging. The rhodium catalytic moiety was then introduced to the reaction mixture as a solution of bis(norbornadiene)rhodium-(I) tetrafluoroborate (catalogue no. 45-0230, Strem Chemicals) in minimal acetone to yield a concentration of 5.5 mM. The resulting solution was vigorously shaken and acetone was removed under vacuum and argon purging at room temperature.

Diethyl [1-^{13}C, 2,3-d_2]fumarate was added by injecting the compound neat into the catalyst solution. The syringe was washed twice with catalyst solution by pulling up solution and then injecting into a round-bottom flask to remove all of the diethyl fumarate out of the syringe. The solution of diethyl fumarate and catalyst was then filtered through 0.45 μm cellulose acetate syringe filter (VWR, 28145-481). The filtered solution was then quickly taken up in a 30 mL plastic syringe and used for injection of the desired amount of imaging reagent precursor for each experiment (4 mL) into the reaction chamber of the polarizer. Different final concentrations of diethyl [1-^{13}C, 2,3-d_2]fumarate in catalyst solution were used to optimize polarization transfer pulse sequences, hydrogenation, ^{13}C imaging, and ^{13}C spectroscopy. However, we saw the best imaging and spectroscopy with 20 mM diethyl [1-^{13}C, 2,3-d_2]fumarate in a 9:1 water/D_2O solution, and it was this concentration of hyperpolarized diethyl [1-^{13}C]succinate that was injected into mice unless stated otherwise. Most hydrogenations were done at 60 °C, with 12 bar of parahydrogen gas and using 15 bar of nitrogen to remove the hyperpolarized compound from the reaction chamber. Hydrogenation was complete using these conditions. Aliquots of hydrogenation reactions were analyzed on a Varian 11.7 T NMR instrument, and ^{13}C NMR was performed. The ^{13}C NMR for the catalyst and diethyl [^{13}C]fumarate solution is significantly different before and after hydrogenation. The change in the carbonyl chemical shift from 167.4 ppm (corresponding to diethyl fumarate) to 175.8 ppm (corresponding to diethyl succinate) is easily seen. A resonance at 167.4 ppm was not seen in any of the six reactions tested. Aliquots of 0.5 mL of hyperpolarized, hydrogenated ^{13}C reagent was then injected into the mouse via tail vein. In a few experiments, aliquots of 1 mL of hyperpolarized hydrogenated reagent were injected into a mouse's intraperitoneal cavity.

Magnetic Resonance Scanner and Coils. All magnetic resonance imaging (MRI) and spectroscopy (MRS) of animals or phantoms was performed in an animal 4.7 T MR scanner (Bruker Avance, Bruker AG, Germany) horizontal bore with a $^{1}H/^{13}C$ full body mouse volume coil (Doty Scientific).

Animals. Male BALB/c mice, purchased from Harlan S/D and on average weighing 25 g, were used. All animal experiments were approved by IACUC of Huntington Medical Research Institutes. The mice were anesthetized by 1.5% isoflurane gas with 0.8 L/min oxygen per face mask. The lateral tail vein was catheterized with 30-gauge tubing (MVT-1, Braintree Scientific), attached to a two-foot PE50 extension. A warm-water tail bath produced the vasodilation critical to successful cannulation. The sedated mouse was then placed in a heated cradle within the bore of the MR scanner.

For experiments that required an intraperitoneal (ip) catheter, the anesthetized mouse was subjected to one of two procedures: laparotomy or needle puncture. The laparotomy technique involved a small (2−4 mm) midsagittal abdominal

dx.doi.org/10.1021/ja2040865 | J. Am. Chem.Soc. 2012, 134, 934−943

incision through skin and peritoneum while the mouse laid supine. The tip of a 2-ft PE50 catheter was then placed in the intraperitoneal space under direct visualization. Silk suture then anchored the catheter to skin as well as closed the wound. Alternatively, ip access was affected by passing the PE50 catheter through an 18 gauge needle after a blind, transcutaneous puncture. The abdominal skin was tented upward to avoid visceral injury. Once the needle was withdrawn over the catheter, no suture was necessary to prevent leaks. After either procedure, the mouse was carefully pronated and placed in the magnet.

The needle method became the preferred, more refined approach as it utilized less time and material and created a tighter catheter-to-skin junction. The success of this method is, however, highly operator-dependent; but in our hands, no abdominal organ injury or other untoward complication occurred.

Measuring Polarization. The polarization of diethyl succinate was measured (25−40 s after polarization) in a plastic syringe via ^{13}C spectroscopy with a single scan pulse and acquire sequence with a pulse angle of 45° in MR scanner. To quantify the degree of hyperpolarization, we used the reference of a single scan spectrum of thermally polarized 3 M [1-^{13}C]acetate phantom at 4.7 T using the following formula:

$$\%P_{t=\text{detection}} = \frac{[\text{reference}]}{[\text{polarized}]}\frac{\text{signal(polarized)}}{\text{signal(reference)}}\frac{100\%}{246\,000} \quad (1)$$

where 1/246 600 corresponds to ^{13}C nuclear polarization at 298 K and at 4.7 T, according to the Boltzmann distribution. The degree of hyperpolarization produced in the PHIP polarizer at time zero was back calculated, using the delivery time and spin−lattice relaxation time T_1 of the hyperpolarized agent as follows:

$$\%P_{t=0} = \%P_{t=\text{detection}} \exp\left(\frac{\text{delivery time}}{T_1}\right) \quad (2)$$

The reported % hyperpolarization refers to % $P_{t=0}$.

^{1}H Magnetic Resonance Imaging. Proton anatomic images for mice were obtained with a dual tuned volume coil to allow coregistration of carbon hyperpolarized images with mouse anatomic images. RARE (rapid acquisition with relaxation enhancement)[37] tripilot was used for placement of the animal and MSME (multi slice multi echo)[37] coronal imaging with a range of slice thicknesses (4.5, 7.5, or 15.2 mm) and a field of view (FOV) of either 6 or 7 cm was used for coregistration of carbon hyperpolarized images. Magnetic field homogeneity was adjusted by single voxel proton MRS (PRESS, point resolved spectroscopy)[37] data acquisition approach and the voxel (0.7 × 0.7 × 0.7 cm) of interest was placed just posterior of the kidneys in the animal. The unsuppressed water signal less than 15 Hz half-width was routinely obtained. Shimming was essential for peak resolution in ^{13}C MRS experiments.

^{13}C Magnetic Resonance Spectroscopy. We have found it optimal for in vivo experiments to perform 2−3 successive injections of hyperpolarized reagent (diethyl [^{13}C]succinate), optimizing the use of the rapidly decaying hyperpolarized ^{13}C MR signal in order to obtain information on both anatomic distribution and metabolism of diethyl [^{13}C]succinate. Consecutive ^{13}C MRS was acquired via a pulse and acquire approach with a nonselective Gaussian radio frequency pulse for excitation and usually a pulse angle of 30° unless noted otherwise (bandwidth 25 000 Hz and acquisition size 2048) every 7−8 s for about 1 min after injection of hyperpolarized diethyl succinate into the mouse. The spectroscopy was done before or after a ^{13}C FISP image was taken (described below). Assignments of the ^{13}C spectroscopy peaks were determined by use of experimentally determined chemical shift values of metabolites in a D_2O/water solution at known pH (See ^{13}C Nuclear Magnetic Resonance section). The FID raw data were then processed in either XwinNMR or MestraNova with baseline correction (Berstein polynomial fit), line broadening of 5 Hz, manual phasing, and referenced to the large diethyl succinate peak at 176.4 ppm (see legend on Table 1).

In a few experiments, ^{13}C spectroscopy was performed on animals before and after 3-nitropropionate injection (see Figure 4). The mouse was injected with 10 μmol of hyperpolarized diethyl succinate via iv injection before and after 200 μL ip injection of a basic 5 mg/mL (42 mM) solution of 3-nitropropionate (Sigma−Aldrich) and a 20 min wait. The aqueous solution of 3-nitropropionate was brought to a pH of 8.5 with a drop of 50% NaOH solution.

For T_1 experiments, the decay of the polarized carbon signal using a single 10° pulse every 6 s for a total of 32 scans and a total of 3.2 min was measured on our 4.7 T MR scanner. The decay of the signal is plotted against time, and the inverse of the exponential of the curve is the spin−lattice relaxation time. The amount of polarization consumed by the observation pulse was not taken into account.

^{13}C Magnetic Resonance Imaging. Carbon-13 imaging was done with a Bruker TRUE FISP sequence.[37] Our imaging sequence used TR = 3.3 ms, TE = 1.6 ms, four averages, 32 × 32 matrix, and bandwidth 52 083 Hz. All imaging was done in the MR scanner with a Doty volume coil. Flip angles of 80°, 60°, or 40° were used in the sequence. Coronal imaging was performed with a FOV of 6 or 7 cm, 1−2 slices with dimensions 15.2 mm, and the center slice was always selected to be the same as proton images. Images were then converted into false color in Paravision 3.0.2 software, and only pixels above a certain intensity were used to remove noise from signal. The image was then overlaid on the proton image. No ^{13}C MRI image was seen if hyperpolarized diethyl succinate was not injected.

^{13}C Nuclear Magnetic Resonance. To assign ^{13}C resonances observed in vivo, proton-decoupled ^{13}C NMR of 30 samples containing solutions of different TCA cycle metabolites at concentrations around 30 mM in D_2O and water solution with 0.5% methanol in the sample as a chemical shift reference was performed on a 11.7 T Varian instrument. pH values of samples were adjusted with 356 mM KOH solution and 50 mM phosphate buffer at pH 7.5 and measured on a pH meter. All spectroscopy was performed with 64−256 transients, 60° flip angle, and relaxation delay of 10 s, and all spectra were referenced to methanol peak. The carbonyl assignments for the relevant metabolites and pH of the samples can be seen in Table 1.

RESULTS

Polarization and T_1 Spin−Lattice Relaxation Time. In the parahydrogen-induced polarization (PHIP) method, the radio frequency pulse used to transfer the spin order from ^{1}H nuclei to ^{13}C is essential to getting high polarization percentages. Changes in the pulse width, amplitude, or timing between the proton and carbon radio frequency pulses affect the percent of polarization that is transferred to carbon-13 atom significantly. We generate the radio frequency heteronuclear pulse using the coupling constants for the compound being

dx.doi.org/10.1021/ja2040865 | J. Am. Chem.Soc. 2012, 134, 934−943

Table 1. ^{13}C Chemical Shifts of TCA Cycle Metabolites[a]

^{13}C chemical shift (ppm)	compd	pH
183.0	succinate C1	7.1, 7.5
182.0	succinate C1	5.7
183.0	lactate C1	6.4
182.5	citrate C6	7.0, 7.4
180.5	citrate C6	5.0
181.8	glutamate C5	7.2
181.4	glutamate C5	5.3
181.6	malate C4	7.3
180.8	malate C4	5.0
181.4	isocitrate C1, C5	7.0
180.7	isocitrate C6	7.0
180.4	malate C1	7.3
175.8	malate C1	5.0
179.7	citrate C1, C5	7.0, 7.4
177.4	citrate C1, C5	5.0
178.1	aspartate C4	6.0
174.8	aspartate C1	6.0
175.8	diethyl succinate C1	7.7, 7.4
175.9	diethyl succinate C1	5.7
175.2	fumarate C1	7.3
174.6	fumarate C1	5.0
175.1	glutamate C1	7.2
175.0	glutamate C1	5.3
135.9	fumarate C2	7.3
135.8	fumarate C2	5.0

[a] ^{13}C chemical shifts of aqueous solutions of TCA cycle metabolites at given pH values were experimentally determined on a 11.7 T NMR instrument. All samples were doped with methanol, and chemical shifts were referenced to the methanol peak. On the 4.7 T MR scanner, ^{13}C chemical shift of C-1 of the diethyl succinate referenced to methanol was determined to be 176.4 ppm.

polarized (Figure 1B) as described by Goldman and Johannesson and co-workers.[32] The coupling constants for succinate at acidic pH were initially used[20] to determine the transfer pulse sequence and then manipulated in a similar manner as in ref 34 until high polarization was achieved. The polarization of diethyl succinate was measured against a standard 3 M [1-^{13}C]acetate phantom as described in the Materials and Methods section by use of a single transient. The B_0 magnetic field in the polarizer was calibrated as previously described.[34] We routinely used a B_0 field between 2.00 and 2.02 mT and a transfer pulse with a 2:1 peak-to-peak voltage amplitude ratio of proton to carbon pulse. Polarization percentage increased from 0.19% + 0.06% to 2.1% + 0.6%, or 5000-fold signal enhancement, compared to Boltzmann polarization after optimization (Figure 1D). Our percent polarization could be considered low compared to the polarization percentages reported in the literature for DNP-polarized compounds,[13−17] but this could be because of the difference in measurement technique. Regardless of the percent polarization, we can image and perform spectroscopy with hyperpolarized diethyl [1-^{13}C]succinate for the same length of time and have comparable signal-to-noise ratios to DNP-polarized compounds.[13−17]

PHIP polarization on a ^{13}C-labeled compound relaxes quickly and the rate is defined by T_1. The spin−lattice relaxation time T_1 for hyperpolarized diethyl succinate in a syringe and in vivo was measured on a 4.7 T MR scanner by measuring the decay of the polarized carbon signal. We are conservative on our assessment of the apparent T_1 and did not take into account the amount of polarization consumed by the observation pulses. T_1 of the labeled carbonyl of a 9:1 water/D_2O solution of 20 mM hyperpolarized diethyl succinate is 38 ± 4 s in vivo and 54 ± 2 s in the syringe. T_1 is significantly lower when polarization occurs in 100% water (24 s in vivo). Due to the longer T_1 occurring in the 9:1 mixture of water/D_2O, this solvent mixture was used in all in vivo experiments. The pH of 20 mM diethyl [^{13}C]fumarate in 9:1 water/D_2O catalyst solution is 8. After hydrogenation, the final pH is 6, arising from the rhodium catalyst degrading into a rhodium hydroxide complex.[39] An in vivo T_1 of 38 s is comparable to other hyperpolarized compounds and gives us more than 3 min ($5T_1$) to image the compound. The final pH of 6 is significantly closer to physiological pH than 2.35 or 11, which were used in our previous succinate polarization experiments.[20]

In Vivo ^{13}C Spectroscopy and Imaging. Real-time detection of metabolism of diethyl succinate was seen in 13 mice injected with 10 μmol of hyperpolarized diethyl succinate via tail vein and in three mice injected with 20 μmol of hyperpolarized diethyl succinate in the peritoneum. In most cases, it took 40−50 s after polarization for hyperpolarized diethyl succinate to be administered to the animal and imaging/spectroscopy to begin. Representative ^{13}C MRS exams of diethyl succinate metabolism in mice can be seen in Figures 2 and 3. Metabolites are seen almost instantly and metabolism can easily be monitored. All spectroscopy shown was collected with a single 30° pulse and acquire sequence every 5−9 s. The time values were determined on the basis of time stamps of the raw data and amount of time the pulse and acquire sequence takes to complete (5 s). The time values correspond to the time elapsed between injection of the hyperpolarized compound and when the spectroscopy was performed. Metabolic products from hyperpolarized diethyl [^{13}C]succinate (the largest peak, labeled DS) were detected within 5 s of the injection of the hyperpolarized substance and persisted for approximately 1 min. All spectra are referenced to the diethyl succinate peak (176.4 ppm), which was referenced in phantom experiments to ^{13}C-labeled methanol. In most animals, no signal was seen in ^{13}C spectroscopy with a single transient if hyperpolarized compound was not injected. ^{13}C spectra using a single transient in a few noninjected mice include natural-abundance ^{13}C lipid peaks at around 30−35 ppm. To determine the chemical identity of the in vivo metabolites observed, we performed several proton-decoupled ^{13}C NMR experiments on a 11.7 T Varian instrument with methanol (49.50 ppm)[40] as a chemical shift reference of samples containing known TCA cycle metabolites in water and D_2O at particular pHs. Some of the data can be seen in Table 1. On the basis of these experiments, we believe that after injection diethyl succinate is metabolized by esterase in the cell and then metabolized to succinate, aspartate, malate, and fumarate.

The pattern of the resonances, as well as the tentative assignments by chemical shift, strongly suggests that diethyl [^{13}C]succinate hyperpolarized by the PHIP technique is metabolized in vivo and that its metabolites retain a significant fraction of the hyperpolarized ^{13}C nuclei through three or more enzyme-catalyzed biochemical reactions. Metabolism of hyperpolarized diethyl succinate was confirmed by ^{13}C MRS in 13 animals via iv injection with 10 μmol of compound and in three mice via ip injection with 20 μmol of hyperpolarized diethyl succinate. Metabolism was observed in all animals. As is very frequently the case for in vivo ^{13}C MRS, there are some slight discrepancies between experiments, mostly attributable to

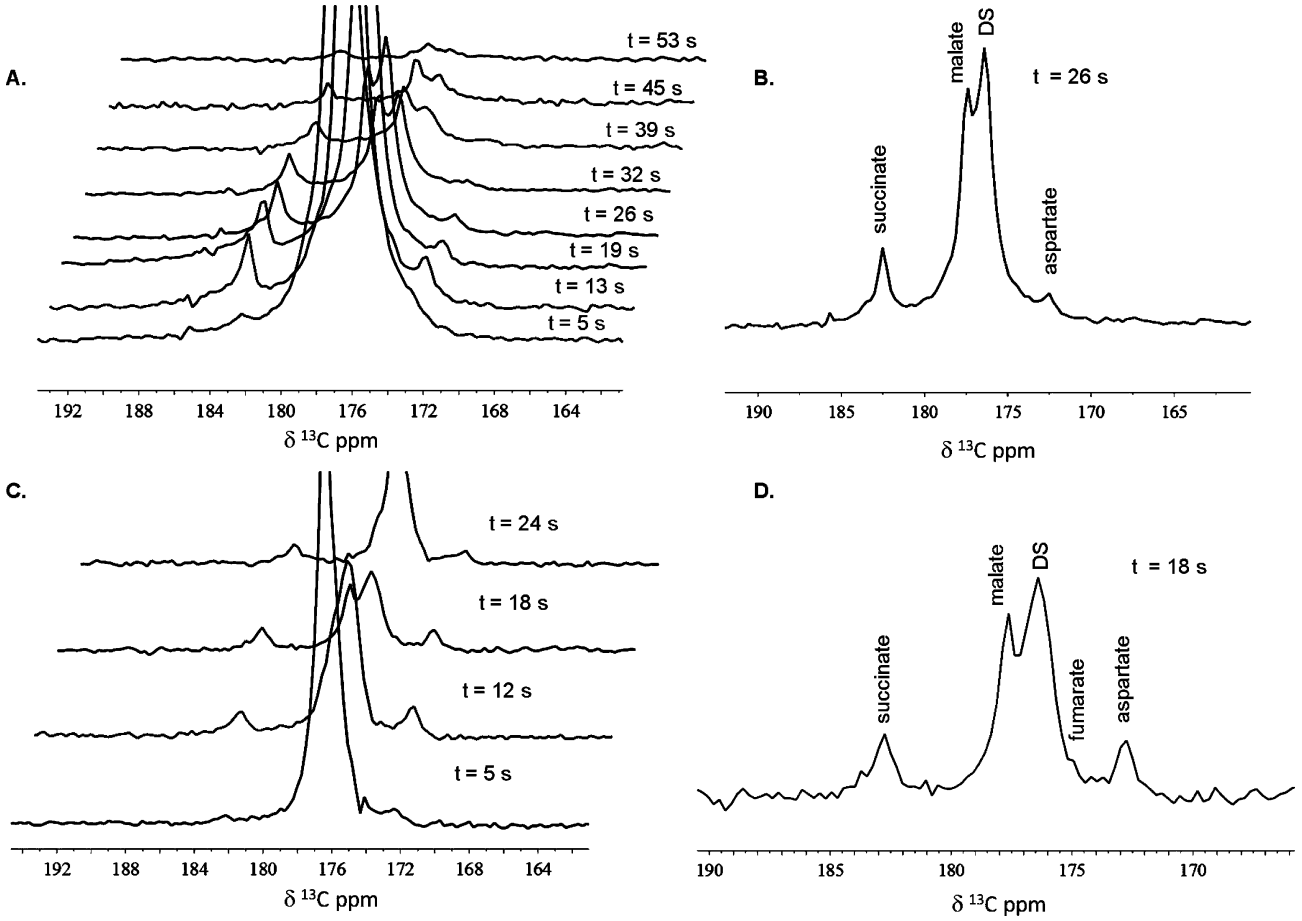

Figure 2. ^{13}C spectroscopy in vivo (iv injection). (A, C) Representative ^{13}C MR time-resolved stackplots as seen in two different mice that received 10 μmol of hyperpolarized diethyl succinate by tail vein injection. All spectroscopy shown was collected with a single 30° pulse and acquire sequence every 5−9 s. Time values correspond to the time elapsed between injection of the hyperpolarized compound and when the spectroscopy was performed. Metabolic products from hyperpolarized ^{13}C diethyl succinate (the largest peak, labeled DS) were detected within 5 s of injection of the hyperpolarized substance and persisted through 53 s. (B) Enlarged view of the region of interest of the ^{13}C MRS acquired at t = 26 s as seen in stackplot A. By use of the diethyl succinate peak as a reference and set to 176.4 ppm, the three distinct resonances are assigned to malate, succinate, and aspartate. (D) Enlarged view of the region of interest of the ^{13}C MRS acquired at t = 18 s as seen in stackplot C. The four distinct resonances are assigned to malate, succinate, fumarate, and aspartate.

differences between one animal and the next. In addition, because of the dynamic state of in vivo metabolism, the peaks and the heights of these peaks are highly dependent on when the spectroscopy was done relative to when the compound was injected. In Figure 3A, the spectroscopy was taken 5−25 s after injection, while in Figure 3B, the spectroscopy was taken 29−43 s after injection.

We have not determined the in vivo flux rate of the TCA cycle from our spectroscopy data for a number of reasons. On the basis of our prior experience with in vivo NMR metabolic rate calculations, a key requirement is that "steady-state" conditions prevail.[41,42] Diethyl succinate, which is not an endogenous substance, at concentrations of 10−20 μmol is a substrate rather than a tracer in relation to the intrinsic concentration of succinate around 0.1 μM. We did not achieve steady-state conditions in the experiments described here. In addition, there are a number of other uncontrolled and uncontrollable variables: differing T_1 values for substrate and metabolic products, decay of polarization under the influence of imaging radio frequency pulses applied, chemical exchange, and other factors, all of which complicate a consistent approach for determining the TCA flux rate. However, knowledge of the precise flux data for diethyl succinate metabolism might not be needed in diagnostic imaging of disease states known to have inhibited or unusual TCA cycle metabolism.

To further explore the metabolism of hyperpolarized diethyl [1-^{13}C, 2,3-d_2]succinate in a mouse, we performed spectroscopy experiments with diethyl succinate before and after ip injection of 3-nitropropionate in four mice. 3-Nitropropionate is a known irreversible inhibitor of succinate dehydrogenase.[35] The metabolism of hyperpolarized diethyl succinate changes after 3-nitropropionate injection (Figure 4). Figure 4A is the ^{13}C spectrum of diethyl succinate metabolism injected by iv after 12 s. Figure 4B is the ^{13}C spectroscopy of an iv injection of hyperpolarized diethyl succinate in the same animal after being treated with 200 μL of 3-nitropropionate solution and waiting 20 min. On the basis of chemical shifts, the downfield succinate resonance is significantly reduced in the animal after 3-nitropropionate treatment. Three out of the four mice demonstrated a reduction to complete loss of the succinate peak after 3-nitropropionate treatment.

Carbon-13 imaging was accomplished by use of the Bruker TRUE FISP imaging sequence[37] in a volume coil on a 4.7 T MR scanner. Given that the gradient rise time of our MR Bruker scanner is 250 μs, the slice thickness for the images is 15.2 mm and the field of view (FOV) is either 6 or 7 cm. We

dx.doi.org/10.1021/ja2040865 | J. Am. Chem.Soc. 2012, 134, 934−943

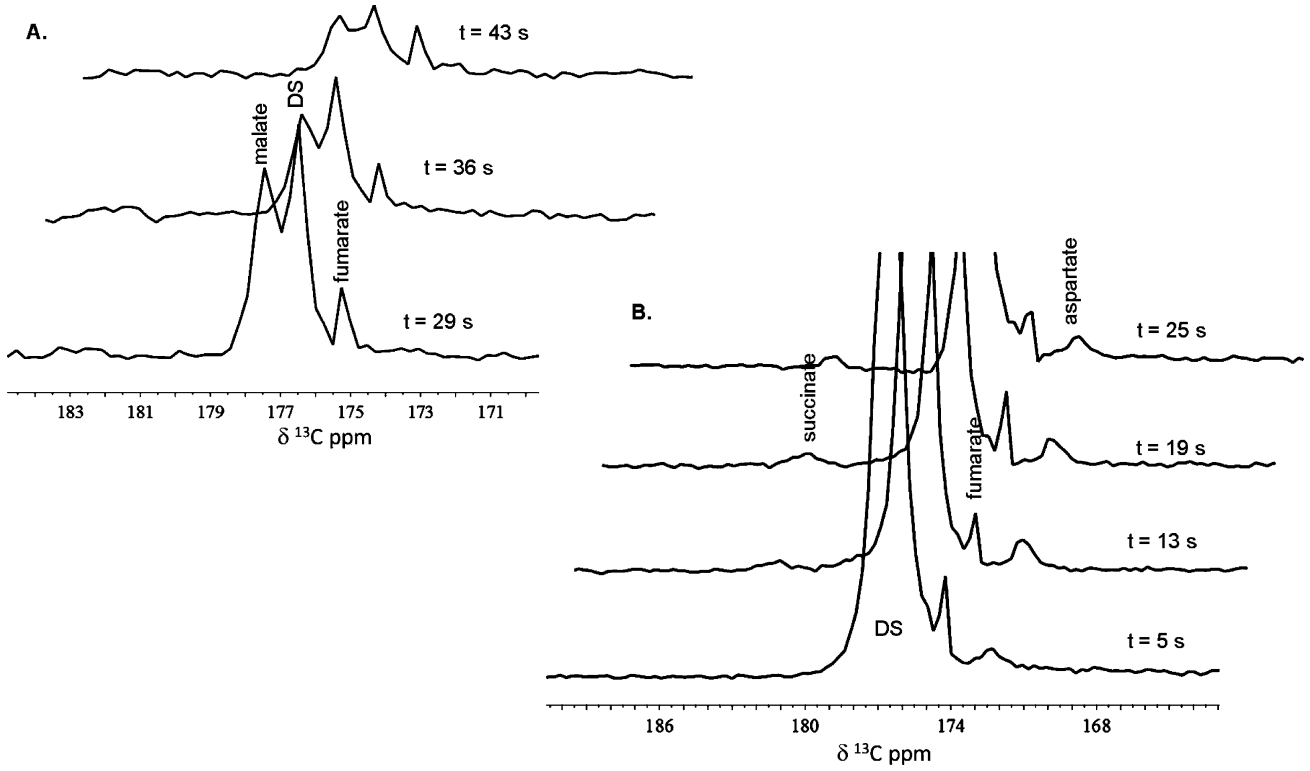

Figure 3. ^{13}C spectroscopy in vivo (ip injection). Panels A and B show ^{13}C MR stackplots for two different mice, each of which received 20 μmol of hyperpolarized diethyl succinate into the peritoneum. Metabolic products from hyperpolarized diethyl [^{13}C]succinate (the largest peak, labeled DS) were detected within 5 s of the injection of the hyperpolarized substance (stackplot B) and persisted for about a minute (stackplot A). By use of the diethyl succinate peak as a reference, two to three distinct resonances can be detected and are assigned to malate, fumarate, succinate, and aspartate.

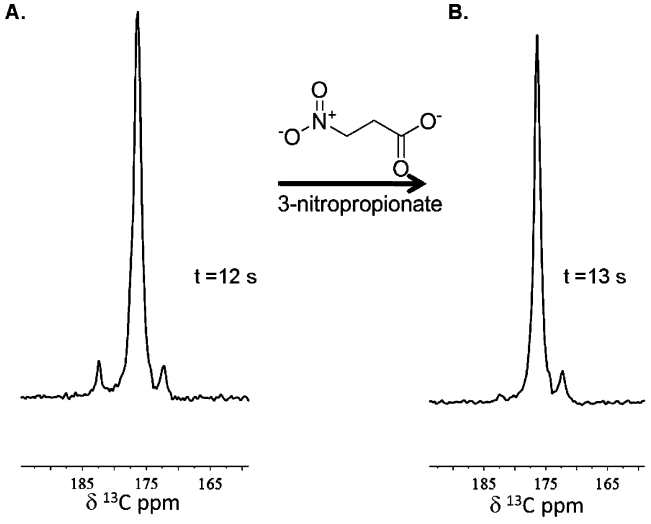

Figure 4. 3-Nitropropionate inhibition. ^{13}C MRS spectra illustrating diethyl succinate metabolism in an animal (A) before and (B) after 3-nitropropionate treatment are shown. The mouse was injected with 10 μmol of hyperpolarized diethyl succinate via iv injection before and after injection of a 3-nitropropionate solution. The downfield resonance corresponding to succinate is significantly reduced in spectrum B compared to spectrum A.

can determine the relative location of hyperpolarized diethyl succinate and its metabolites in the animal when injected via tail vein or into the peritoneum via ^{13}C FISP imaging. At the beginning of this work, a flip angle of 80° was used for ^{13}C imaging, but, we have been able to image for longer intervals and preserve the signal with flip angles of 60° and 40°. We can image every 9 s for up to 1 min with the TRUE FISP sequence with 60° and 40° flip angles. No ^{13}C image is seen if hyperpolarized compound is not injected. Overlays of ^{13}C FISP images in false color over the proton image of the animal with the same FOV and central slice placement are displayed in Figure 5. On the basis of the overlays of the images, diethyl succinate when injected iv into a mouse seems to quickly go through the cardiovascular system, as seen in Figure 5A,B, where the FISP image is in the location of the heart, and then we believe the hyperpolarized molecule collects in the bladder and ureters (Figure 5B) based on the proximity of the FISP images to the kidneys seen in proton MRI images. With intraperitoneal injection, the hyperpolarized compound and its metabolites appear to remain in the peritoneum (Figure 5C,D). Other fast imaging sequences, fast imaging employing steady-state acquisition (FIESTA)[21] or fast low-angle shot (FLASH),[43] that were not used in this study might give better spatial resolution than the TRUE FISP sequence. In the future, we plan on using different ^{13}C imaging sequences to improve our spatial resolution.

■ DISCUSSION

In this study, we have been able to synthesize, polarize, and image diethyl [1-^{13}C, 2,3-d_2]succinate. Diethyl succinate can be hyperpolarized in our polarizer in an aqueous solution, with signal enhancement of 5000 compared to Boltzmann polarization, and the hyperpolarized solution can be generated at 4 min intervals with complete conversion to diethyl succinate. T_1 of hyperpolarized ^{13}C-labeled carbonyl in diethyl succinate was determined to be 38 s in vivo, which allows for the signal to be measured for over 3 min. ^{13}C MRS and MRI were achieved

dx.doi.org/10.1021/ja2040865 | J. Am. Chem.Soc. 2012, 134, 934−943

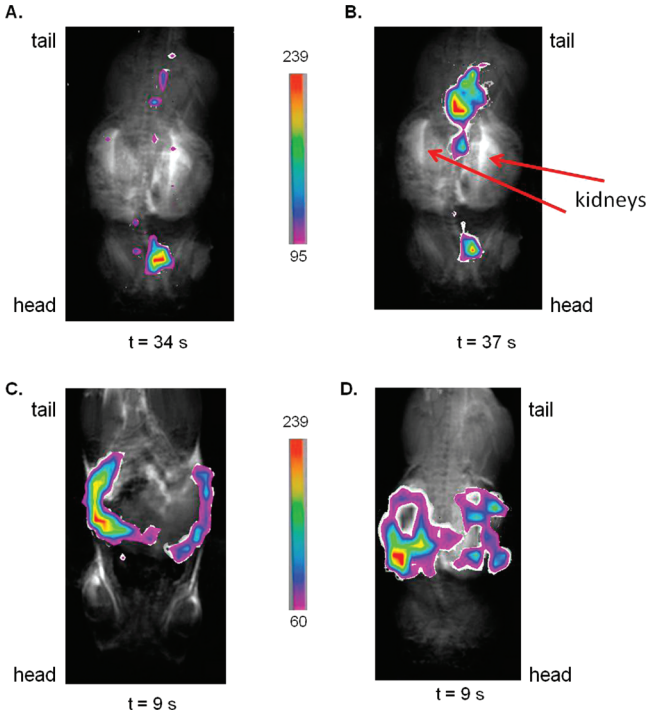

Figure 5. ^{13}C imaging in vivo. Images A–D are overlays of ^{13}C FISP images (60° flip angle) in false color taken of different injections of hyperpolarized diethyl succinate over the proton image of the mouse with the same 6 cm FOV, central slice placement, and slice thickness. To remove noise from FISP images, only pixels above a certain threshold were used. The scales corresponding to each set of false color images are seen. Time values below the images show the amount of time (in seconds) after injection of the hyperpolarized compound that the ^{13}C image was taken. Images A and B are ^{13}C FISP images of two different iv injections of hyperpolarized diethyl succinate. On the basis of the location of the ^{13}C image in images A and B, some of the hyperpolarized compound and its metabolites are localized around the region of the heart. In image B, the majority of the hyperpolarized signal is found posterior to the kidneys in the region of the bladder and ureters. Images C and D are overlays of ^{13}C FISP images of two different ip injections of hyperpolarized diethyl succinate. On the basis of the location of the ^{13}C images, the hyperpolarized compound seems to be retained in the peritoneum with ip injection in the time window of the image (9 s).

in vivo by tail vein and intraperitoneal injections of 20 mM hyperpolarized diethyl succinate into normal mice. Metabolism of the compound was seen in all injections. On the basis of ^{13}C MRS TCA cycle metabolite phantoms, we have assigned the spectral peaks in our in vivo studies of hyperpolarized diethyl succinate to be malate, succinate, fumarate, and aspartate (Figures 2 and 3). The metabolism of diethyl succinate was altered after exposure of the animal to 3-nitropropionate, a known irreversible inhibitor of succinate dehydrogenase (Figure 4). On the basis of our results, parahydrogen-induced polarized diethyl succinate allows for ultrafast in vivo MRI and MRS with a high signal-to-noise ratio, and multiple enzyme-catalyzed reactions can be visualized.

Reduction of hyperpolarized succinate was seen in multiple studies after inhibition of succinate dehydrogenase by the inhibitor 3-nitropropionate. This is counterintuitive to what one would expect and could be due to several reasons. First, while 3-nitropropionate inhibits succinate dehydrogenase when presented to the purified enzyme, this does not exclude additional effects of the inhibitor in vivo.[44] Second, we have no information concerning the behavior of intramitochondrial succinate dehydrogenase in the presence of high excess of a succinate analogue like diethyl succinate. In addition, hyperpolarized metabolic events, which permit the close observation of metabolic regulation in vivo during the first 100 s after equilibrium is challenged by substrate or inhibitor, have never before been studied.

In the studies described, the rhodium hydrogenation catalyst was not removed before injection of hyperpolarized diethyl succinate. On the basis of concentration, 2.75 μmol (iv) and 5.5 μmol (ip) of catalyst was injected into the mice with each injection. The animals seemed to tolerate multiple injections of hyperpolarized diethyl succinate and hydrogenation catalyst. However, we do realize that for the technique to be used in patients in clinical studies, sterile methods for removing the catalyst must be developed. We are in the process of attaching the rhodium catalyst to a solid support, removing the catalyst after hydrogenation through the use of cationic resins that will remove the cationic catalyst and via fast filtration.

Hyperpolarized diethyl succinate has several advantages compared to DNP-hyperpolarized [1-^{13}C]pyruvate and PHIP-hyperpolarized [1-^{13}C]succinate. Using PHIP, hyperpolarization of diethyl succinate can be achieved on a quicker time scale than any DNP-hyperpolarized compound so far reported. We can easily generate 20 different samples of hyperpolarized diethyl succinate in a single day for in vivo imaging experiments. The PHIP method of hyperpolarization allows for multiple injections of hyperpolarized compound in the same animal. All animals in this study were injected 3–4 times with hyperpolarized diethyl succinate, which allowed us to do over 40 different ^{13}C MRS and MRI experiments. In addition, the 4-min time interval for hyperpolarization with PHIP allows metabolism to be quickly monitored in the same animal before and after treatment with a compound (for example, 3-nitropropionate). This would allow the monitoring of metabolism in disease animal models before and after drug treatment (for example, chemotherapeutics) on a time scale of seconds to minutes. T_1 of hyperpolarized diethyl succinate is significantly longer (38 s in vivo) than that of hyperpolarized [1-^{13}C]pyruvate (20–15 s in vivo), allowing for in vivo studies of longer duration and more physiological concentrations of metabolic imaging reagents.[14] In this study, a 20 mM solution of hyperpolarized diethyl succinate is being used with 500 μL–1 mL injection volumes, which is quite comparable to the concentrations used with DNP-polarized pyruvate. The lowest concentration of injected hyperpolarized [1-^{13}C]pyruvate in a mouse is reported at 10 mM;[16] however, most papers report higher concentrations.[13−15] Multiple steps of metabolism can be observed with hyperpolarized diethyl succinate, unlike hyperpolarized [1-^{13}C]pyruvate.

Hyperpolarized diethyl succinate has several advantages over hyperpolarized succinate, the first physiological PHIP reagent developed in our laboratory.[20,30] It is known that the dicarboxylic acid succinate is only poorly transported across many biological membranes and in particular barely crosses the mitochondrial membrane to gain access to TCA cycle enzymes involved in metabolism.[23,24] Diethyl succinate is taken up and metabolized in seconds in our in vivo studies. In addition, we can hyperpolarize diethyl succinate under more physiological conditions, notably pH close to biological neutrality, compared to the acidic or basic conditions needed to polarize succinate.[20] With PHIP-polarized diethyl succinate's long T_1, physiological pH, ability to cross biological membranes, and high signal-to-noise

dx.doi.org/10.1021/ja2040865 | J. Am. Chem.Soc. 2012, 134, 934–943

ratio with only a 20 mM solution; this compound has the potential of studying metabolism in a variety of diseases.

In the future, we are planning on using hyperpolarized diethyl succinate to study metabolism in cancer and neurodegenerative disease animal models. Rapid visualization of the first minute of the TCA cycle in normal or cancerous tissues may throw new light on the regulation of this pathway previously beyond the limits of detection by conventional in vivo NMR. In addition, we plan on injecting hyperpolarized diethyl succinate in the carotid artery of an animal to determine if the molecule will cross the blood–brain barrier (BBB). Hyperpolarized succinate does not cross the BBB in normal healthy animals,[30] and it is known that hyperpolarized ethyl pyruvate crosses the BBB significantly better than hyperpolarized pyruvate.[15] Based on the ability of noncharged compounds to cross the BBB, there is a definite possibility that hyperpolarized diethyl succinate will cross the blood–brain barrier, which would allow us to compare metabolism of the compound in normal animals versus neurodegenerative disease animal models.

In summary, we have developed a more flexible hyperpolarized molecular imaging reagent that can be injected at physiological pH, rapidly enters cells and tissues, and is metabolized by enzymes in the TCA cycle. Hyperpolarized diethyl succinate has the potential of being used in clinical metabolic imaging and spectroscopy. Furthermore, this molecule has the promise of exploring metabolic differences in the TCA cycle in both diseased and normal tissue in disease models, providing real-time metabolic fingerprinting of different types of cancers. Early response to targeted cancer therapy and successful outcome can potentially be predicted by the appearance, in otherwise predominantly glycolytic tumors, of the intermediates of a (recovered) TCA cycle. In vivo applications of hyperpolarized diethyl succinate may reveal an entirely new regime wherein the local status of TCA cycle metabolism is interrogated and therapy is monitored in disease models on the time scale of seconds to minutes with unprecedented chemical specificity and MR sensitivity.

■ ASSOCIATED CONTENT

Supporting Information

One figure showing a TCA cycle diagram and one table containing all experiments performed. This material is available free of charge via the Internet at http://pubs.acs.org.

■ AUTHOR INFORMATION

Corresponding Author

pratip@hmri.org

■ ACKNOWLEDGMENTS

We thank the Caltech NMR facility, especially Dr. Scott Ross, who helped us with NMR experiments. In addition, we thank Professor Robert Grubbs at Caltech and his laboratory for the use of a fume hood and chemistry discussions. We thank Meng Wei and Dr. Kent Harris for their help with the polarizer. N.M.Z. thanks the James G. Boswell Foundation for their financial support. The work was supported in part by NIH 1R21 CA118509 (P.B.), NCI 5R01CA122513 (B.D.R.), NIH 1R01NS048589 (B.D.R.), and Tobacco Related Disease Research Program (16KT-0044) (P.B.).

■ REFERENCES

(1) Garber, K. *J. Natl. Cancer Inst.* **2004**, *96*, 1805–1806.
(2) Bayley, J. P.; Devilee, P. *Curr. Opin. Genet. Dev.* **2010**, *20*, 324–329.
(3) Ralph, S. J.; Rodriguez-Enriquez, S.; Neuzil, J.; Moreno-Sanchez, R. *Mol. Aspects Med.* **2010**, *31*, 29–59.
(4) Beal, M. F. *Trends Neurosci.* **2000**, *23*, 298–304.
(5) Bubber, P.; Haroutunian, V.; Fisch, G.; Blass, J. P.; Gibson, G. E. *Ann. Neurol.* **2005**, *57*, 695–703.
(6) Henry, P. G.; Lebon, V.; Vaufrey, F.; Brouillet, E.; Hantraye, P.; Bloch, G. *J. Neurochem.* **2002**, *82*, 857–866.
(7) Brouillet, E.; Guyot, M. C.; Mittoux, V.; Altairac, S.; Conde, F.; Palfi, S.; Hantraye, P. *J. Neurochem.* **1998**, *70*, 794–805.
(8) Ross, B.; Lin, A.; Harris, K.; Bhattacharya, P.; Schweinsburg, B. *NMR Biomed.* **2003**, *16*, 358–369.
(9) Bowers, C. R.; Weitekamp, D. P. *Phys. Rev. Lett.* **1986**, *57*, 2645–2648.
(10) Bowers, C. R.; Weitekamp, D. P. *Solid State Nucl. Magn. Reson.* **1998**, *11*, 123–128.
(11) Kuhn, L. T.; Bargon, J. *Top. Curr. Chem.* **2007**, *276*, 25–68.
(12) Golman, K.; Olsson, L. E.; Axelsson, O.; Mansson, S.; Karlsson, M.; Petersson, J. S. *Br. J. Radiol.* **2003**, *76* (Spec. No. 2), S118–127.
(13) Arunachalam, A.; Whitt, D.; Fish, K.; Giaquinto, R.; Piel, J.; Watkins, R.; Hancu, I. *NMR Biomed.* **2009**, *22*, 867–873.
(14) Golman, K.; in 't Zandt, R.; Thaning, M. *Proc. Natl. Acad. Sci. U.S.A.* **2006**, *103*, 11270–11275.
(15) Hurd, R. E.; Yen, Y. F.; Mayer, D.; Chen, A.; Wilson, D.; Kohler, S.; Bok, R.; Vigneron, D.; Kurhanewicz, J.; Tropp, J.; Spielman, D.; Pfefferbaum, A. *Magn. Reson. Med.* **2010**, *63*, 1137–1143.
(16) Wilson, D. M.; Keshari, K. R.; Larson, P. E.; Chen, A. P.; Hu, S.; Van Criekinge, M.; Bok, R.; Nelson, S. J.; Macdonald, J. M.; Vigneron, D. B.; Kurhanewicz, J. *J. Magn. Reson.* **2010**, *205*, 141–147.
(17) Golman, K.; Zandt, R. I.; Lerche, M.; Pehrson, R.; Ardenkjaer-Larsen, J. H. *Cancer Res.* **2006**, *66*, 10855–10860.
(18) Schroeder, M. A.; Atherton, H. J.; Ball, D. R.; Cole, M. A.; Heather, L. C.; Griffin, J. L.; Clarke, K.; Radda, G. K.; Tyler, D. J. *FASEB J.* **2009**, *23*, 2529–2538.
(19) Marjanska, M.; Iltis, I.; Shestov, A. A.; Deelchand, D. K.; Nelson, C.; Ugurbil, K.; Henry, P. G. *J. Magn. Reson.* **2010**, *206*, 210–218.
(20) Chekmenev, E. Y.; Hovener, J.; Norton, V. A.; Harris, K.; Batchelder, L. S.; Bhattacharya, P.; Ross, B. D.; Weitekamp, D. P. *J. Am. Chem. Soc.* **2008**, *130*, 4212–4213.
(21) Bhattacharya, P.; Harris, K.; Lin, A. P.; Mansson, M.; Norton, V. A.; Perman, W. H.; Weitekamp, D. P.; Ross, B. D. *Magn. Reson. Mater. Phys., Biol. Med.* **2005**, *18*, 245–256.
(22) Bhattacharya, P.; Chekmenev, E. Y.; Reynolds, W. F.; Wagner, S. R.; Zacharias, N.; Chan, H. R.; Bunger, R.; Ross, B. D. *NMR Biomed.* **2011**, *24*, 1023–1028.
(23) Nishiitsutsuji-Uwo, J. M.; Ross, B. D.; Krebs, H. A. *Biochem. J.* **1967**, *103*, 852–862.
(24) Jans, A. W.; Willem, R. *Eur. J. Biochem.* **1991**, *195*, 97–101.
(25) Isaacs, J. S.; Jung, Y. J.; Mole, D. R.; Lee, S.; Torres-Cabala, C.; Chung, Y. L.; Merino, M.; Trepel, J.; Zbar, B.; Toro, J.; Ratcliffe, P. J.; Linehan, W. M.; Neckers, L. *Cancer Cell* **2005**, *8*, 143–153.
(26) Selak, M. A.; Armour, S. M.; MacKenzie, E. D.; Boulahbel, H.; Watson, D. G.; Mansfield, K. D.; Pan, Y.; Simon, M. C.; Thompson, C. B.; Gottlieb, E. *Cancer Cell* **2005**, *7*, 77–85.
(27) Ladriere, L.; Zhang, T. M.; Malaisse, W. J. *JPEN, J. Parenter. Enteral Nutr.* **1996**, *20*, 251–256.
(28) Malaisse, W. J.; Zhang, T. M.; Verbruggen, I.; Willem, R. *Biochem. J.* **1996**, *317* (Pt3), 861–863.
(29) Diethyl Succinate, MSDS No. 112402 [Online]; Sigma-Aldrich, St. Louis, MO, July 21, 2010. http://www.sigmaaldrich.com/catalog/DisplayMSDSContent.do (Accessed March 1, 2011).
(30) Bhattacharya, P.; Chekmenev, E. Y.; Perman, W. H.; Harris, K. C.; Lin, A. P.; Norton, V. A.; Tan, C. T.; Ross, B. D.; Weitekamp, D. P. *J. Magn. Reson.* **2007**, *186*, 150–155.
(31) Imamoto, T. *Pure Appl. Chem.* **2001**, *73*, 373–376.

(32) Goldman, M.; Johannesson, H.; Axelsson, O.; Karlsson, M. *Magn. Reson. Imaging* **2005**, *23*, 153−157.
(33) Hovener, J. B.; Chekmenev, E. Y.; Harris, K. C.; Perman, W. H.; Robertson, L. W.; Ross, B. D.; Bhattacharya, P. *Magn. Reson. Mater. Phys., Biol. Med.* **2009**, *22*, 111−121.
(34) Hovener, J. B.; Chekmenev, E. Y.; Harris, K. C.; Perman, W. H.; Tran, T. T.; Ross, B. D.; Bhattacharya, P. *Magn. Reson. Mater. Phys., Biol. Med.* **2009**, *22*, 123−134.
(35) Alston, T. A.; Mela, L.; Bright, H. J. *Proc. Natl. Acad. Sci. U.S.A.* **1977**, *74*, 3767−3771.
(36) Sun, F.; Huo, X.; Zhai, Y.; Wang, A.; Xu, J.; Su, D.; Bartlam, M.; Rao, Z. *Cell* **2005**, *121*, 1043−1057.
(37) Bernstein, M. A.; King, K. F.; Zhou, X. J. *Handbook of MRI Sequences*; Elsevier Academic Press: San Diego, CA, 2004.
(38) Brooks, M. A.; Chan, T. H. *Synthesis* **1983**, *3*, 201−203.
(39) Evans, D. A.; Miller, S. J.; Brown, J. M.; Layzell, T. P.; Ramsden, J. A. In *Handbook of Reagents for Organic Synthesis: Chiral reagents for asymmetric synthesis*; John Wiley and Sons: West Sussex, England, 2003; pp 76−81.
(40) Gottlieb, H. E.; Kotlyar, V.; Nudelman, A. *J. Org. Chem.* **1987**, *62*, 7512−7515.
(41) Sailasuta, N.; Tran, T. T.; Harris, K. C.; Ross, B. D. *J. Magn. Reson.* **2010**, *207*, 352−355.
(42) Sailasuta, N.; Abulseoud, O.; Harris, K. C.; Ross, B. D. *J. Cereb. Blood Flow Metab.* **2010**, *30*, 950−960.
(43) Golman, K.; Axelsson, O.; Johannesson, H.; Mansson, S.; Olofsson, C.; Petersson, J. S. *Magn. Reson. Med.* **2001**, *46*, 1−5.
(44) Saad, L. O.; Mirandola, S. R.; Maciel, E. N.; Castilho, R. F. *Neurochem. Res.* **2006**, *31*, 541−548.